

INTERNATIONAL UNION OF PURE
AND APPLIED CHEMISTRY

ANALYTICAL CHEMISTRY DIVISION
COMMISSION ON SPECTROCHEMICAL AND
OTHER OPTICAL PROCEDURES FOR ANALYSIS*

Nomenclature, Symbols, Units, and their Usage in Spectrochemical Analysis—XVIII

**LASER-BASED MOLECULAR SPECTROSCOPY FOR
CHEMICAL ANALYSIS—RAMAN SCATTERING
PROCESSES**

(IUPAC Recommendations 1997)

Prepared for publication by

B. SCHRADER¹ AND D. S. MOORE²

¹Institut für Physikalische und Theoretische Chemie, Universität-GH-Essen, D-45117 Essen, Germany

²Chemical Science and Technology Division, Los Alamos National Laboratory, Los Alamos, NM 87544, USA

*Membership of the Commission during the period 1987–1995 in which the report was prepared was as follows:

Chairman: 1987–1991 J.-M. M. Mermet (France); 1991–1995 T. Vo-Dinh (USA); *Secretary:* 1987–1989 L. R. P. Butler (South Africa); 1989–1993 A. M. Ure (UK); 1993–1995 D. S. Moore (USA); *Titular Members:* G. Gauglitz (Germany, 1991–95); W. H. Melhuish (New Zealand, 1985–89); J. N. Miller (UK, 1991–95); D. S. Moore (USA, 1989–93); N. S. Nogar (USA, 1987–1991); N. Omenetto (Italy, 1989–91); B. Schrader (Germany, 1989–95); C. Sénémaud (France, 1987–89); N. H. Velthorst (Netherlands, 1993–95); T. Vo-Dinh (USA, 1989–91); M. Zander (Germany, 1987–89); *Associate Members:* F. Adams (Belgium, 1991–95); A. M. Andreani (France, 1991–95); J. R. Bacon (UK, 1993–95); H. J. Coufal (USA, 1989–95); G. Gauglitz (Germany, 1989–91); G. M. Hieftje (USA, 1983–93); T. Imasaka (Japan, 1993–95); W. Lukosz (Switzerland, 1993–95); J. N. Miller (UK, 1989–91); D. S. Moore (USA, 1987–89); N. Omenetto (Italy, 1985–89); B. Schrader (Germany, 1987–89); C. Sénémaud (France, 1989–91); R. Sturgeon (Canada, 1985–91); G. C. Turk (1993–95); N. H. Velthorst (Netherlands, 1989–93); T. Vo-Dinh (USA, 1987–89); J. Wilkinson (UK, 1993–95); J. P. Willis (South Africa, 1985–91); E. Yeung (USA, 1987–95); *National Representatives:* K. Danzer (GDR, 1985–91); K. Zimmer (Hungary, 1985–89); S. Shibata (Japan, 1985–95); L. Pszxonicki (Poland, 1985–91); D. Z. Batistoni (Argentina, 1987–93); M. Valcarcel (Spain, 1987–95); B. Gilbert (Belgium, 1989–91); I. Rubeska (Czech Republic, 1989–91); L. Bezur (Hungary, 1989–91); A. K. De (India, 1989–93); A. Ulubelen (Turkey, 1989–95); P. S. Zacharias (India, 1993–95); C. J. Rademeyer (South Africa, 1993–95); K. Volka (Czech Republic, 1993–95); A. J. Curtius (Brazil, 1993–95); J. Park (South Korea, 1993–95).

Republication or reproduction of this report or its storage and/or dissemination by electronic means is permitted without the need for formal IUPAC permission on condition that an acknowledgement, with full reference to the source along with use of the copyright symbol ©, the name IUPAC and the year of publication are prominently visible. Publication of a translation into another language is subject to the additional condition of prior approval from the relevant IUPAC National Adhering Organization.

Nomenclature, symbols, units, and their usage in spectrochemical analysis—XVIII. Laser-based molecular spectroscopy for chemical analysis: Raman scattering processes (IUPAC Recommendations 1997)

Synopsis: This report is 18th in a series on Spectrochemical Methods of Analysis issued by IUPAC Commission V.4. It is concerned with Raman scattering processes, usually induced by lasers, covering the UV, visible, and near infrared spectral regions. Raman scattering can be divided into linear and non linear processes. Due to their importance for chemical analysis, mainly the linear Raman effects are treated.

CONTENTS:

1 INTRODUCTION

- 1.1 Preceding documents
- 1.2 Basic Raman scattering terms

2 MOLECULAR VIBRATIONS

3 METHODS OF OBSERVING MOLECULAR VIBRATIONS

- 3.1 Infrared absorption
- 3.2 Raman scattering
- 3.3 Fluorescence

4 THE RAMAN SPECTRUM

- 4.1 Raman frequencies
- 4.2 Anharmonicity
- 4.3 Raman intensities

5 NON-CLASSICAL RAMAN EFFECTS

- 5.1 Resonance Raman effect
- 5.2 Surface-enhanced Raman effect
- 5.3 Non-linear Raman effects

6 RECORDING OF RAMAN SPECTRA

- 6.1 Raman spectrometers
- 6.2 The radiant power of Raman scattered radiation
- 6.3 Influence of the optical properties of the sample
 - 6.3.1 Liquid samples
 - 6.3.2 Powder samples
- 6.4 Influence of thermal emission
- 6.5 Influence of fluorescence and phosphorescence
- 6.6 Special sample arrangements
 - 6.6.1 Non-absorbing powders
 - 6.6.2 Absorbing samples
- 6.7 Presentation of Raman spectra

7 INDEX OF TERMS

8 REFERENCES

1 INTRODUCTION

1.1 Preceding documents

A series of documents dealing with nomenclature, symbols and units used in spectrochemical analysis has been issued by IUPAC:

Part I [*Pure Appl. Chem.*, **30**, 653–679 (1972)] is concerned mainly with general recommendations in the field of emission spectrochemical analysis.

Part II [*Pure Appl. Chem.*, **45**, 99–103 (1976)] gives some basic rules on data interpretation.

Part III [*Pure Appl. Chem.* **45**, 105–123 (1976),] deals extensively with the nomenclature of analytical flame (atomic emission and absorption) spectroscopy and associated procedures.

Part IV [*Pure Appl. Chem.* **52**, 2541–2552 (1980)] concerns X-ray emission (and fluorescence) spectroscopy.

Part V [*Pure Appl. Chem.* **57**, 1453–1490 (1985)] deals with the classification and description of radiation sources.

Part VI [*Pure Appl. Chem.* **56**, 231–345 (1984)] covers molecular luminescence spectroscopy.

Part VII [*Pure Appl. Chem.* **60**, 1449–1460 (1988)] is concerned with molecular absorption spectroscopy (UV/VIS).

Part VIII [*Pure Appl. Chem.* **63**, 735–746 (1991)] deals with a new nomenclature system for X-ray spectroscopy.

Part IX [*Pure Appl. Chem.* **67**, 1725–1744 (1995)] covers fundamental aspects of spectral dispersion and isolation of radiation.

Part X [*Pure Appl. Chem.* **60**, 1461–1472 (1988)] deals with sample preparation for analytical atomic spectroscopy and other related techniques.

Part XI [*Pure Appl. Chem.* **67**, 1745–1760 (19945)] deals with the detection of radiation.

Part XII [*Pure Appl. Chem.* **64**, 253–259, 1992] deals with terms related to electrothermal atomization.

Part XIII [*Pure Appl. Chem.* **64**, 261–264, 1992] deals with terms related to chemical vapour generation.

Part XIV [*Pure Appl. Chem.*] presents a new IUPAC Notation for laser-based atomic spectroscopy.

Part XV [*Pure Appl. Chem.* **67**, 1913–1928 (1995)] deals with the fundamental properties of lasers used in laser-based molecular spectroscopy for chemical analysis.

Part XVI [*Pure Appl. Chem.*] deals with laser-based molecular luminescence techniques for chemical analysis.

Part XVII [*Pure Appl. Chem.*] deals with laser-based molecular absorption techniques for chemical analysis.

Many of the terms discussed in this document are related to previous documents, namely the general symbols defined in Parts I, VI, VII, IX, XI, and especially XV, XVI and XVII. Parts I - XIII and their index are also available electronically via <http://chem.rsc.org/rsc/iupac/iupacv4/specanhp.htm>.

1.2 Basic Raman scattering terms

A *scattering process* is an interaction of a *primary light quantum* with atoms, molecules, or their aggregates as crystals, by which a *secondary light quantum* is produced, with a different phase and polarization and maybe another energy when compared to that of the primary light quantum. The scattering process occurs with an extremely short time delay.

An *elastic scattering process* produces radiation with the same energy as that of the primary light. Depending on the size of a scattering particle and its refractive index relative to that of the surrounding medium, the processes are called *Rayleigh*, *Mie* or *Tyndall scattering*. Specular reflection can occur from large particles. Further, for collections of particles, processes of *multiple reflection*, *refraction*, and *diffraction of powders* may cause *diffuse reflection* or *diffuse scattering*.

An *inelastic scattering process* produces secondary light quanta with different energy. One such process is the Raman effect. During the interaction of the primary light quantum with a molecule or crystal, the energy of vibrational and/or rotational states may be exchanged and a secondary light quantum of lower or higher energy is emitted. The energy difference is equal to the *vibrational energy* E_{vib} of a molecule or crystal and/or the *rotational energy* E_{rot} of a molecule. It may be recorded, if monochromatic radiation is used for the primary excitation, as a *vibrational*, *rotational* or *rotation-vibration Raman spectrum*. The inelastic interaction of a primary light quantum with a molecule or crystal in its rotational or vibrational

ground state produces the *Stokes Raman spectrum*, a red-shifted spectrum. Due to thermal excitation according to the Boltzmann equation, some molecules are in their vibrational (or rotational) excited states. The interaction of the primary light with these molecules may produce a blue-shifted Raman spectrum, the *anti-Stokes Raman spectrum*. The relative intensity of the Raman lines in the Stokes and anti-Stokes Raman spectra may be employed using the Boltzmann equation for the determination of the *vibrational* (or *rotational*) *temperature*.

In addition to the Raman effect, *Brillouin scattering* produces secondary light quanta by interaction with *acoustic waves* in crystals or liquids. Also, the *Doppler effect* due to the interaction with moving particles in a gas or liquid may produce light quanta with different energy as used in *laser Doppler anemometry*.

There are also other processes that produce secondary light quanta with different energies, but they occur with a time delay (longer than the phase relaxation time, see [XVI]) and are not scattering processes. An example is *photoluminescence*, by which a primary light quantum is absorbed and the excited state of the molecule or aggregate of molecules (including liquids; see below) emits, after some delay, a secondary light quantum as *fluorescence*, *delayed fluorescence*, or *phosphorescence* (see [VI]). These processes occur with a larger quantum yield, which may be about 10 orders of magnitude larger than that of a Raman scattering process, and therefore they can interfere with the detection of the Raman signal (see Sec. 6.5).

2 MOLECULAR VIBRATIONS

All motions of the nuclei in a molecule relative to other nuclei in the same molecule can be considered to be a superposition of *normal vibrations* k for which all nuclei are vibrating with the same *normal frequency* ν_k and *normal coordinate* q_k . Polyatomic molecules, having n atoms, possesses $3n-6$ normal vibrations ($3n-5$ when linear). The *fundamental frequencies* of the normal vibrations are dependent on the masses of the nuclei, their geometrical arrangement and the strength of the chemical bonds. In molecular aggregates, the vibrations of the individual components are coupled.

3 METHODS OF OBSERVING MOLECULAR VIBRATIONS

3.1 Infrared absorption

According to quantum mechanics a molecule can take up an amount of energy, the vibrational energy $E_{\text{vib}} = h\nu_k$, to reach higher vibrationally excited states. Light quanta in the infrared region have wavelengths λ of 2.5–1000 μm (wavenumbers 4000–10 cm^{-1}). Molecules may absorb light quanta of these wavelengths, exciting the molecular vibrations and producing an *infrared absorption spectrum*. (see Fig. 1a)

3.2 Raman scattering

The molecules can also be irradiated using monochromatic radiation, the *exciting radiation*, [VI 3.1] from an *excitation source* (usually a laser) in the ultraviolet (UV), visible (VIS), or near-infrared (NIR) region of the spectrum, whose quanta have the energy $h\nu_0$. During the inelastic scattering process, vibrational energy $h\nu_k$ can be exchanged, whereby light quanta are scattered which have a *scattered energy* $h\nu_R = h\nu_0 \pm h\nu_k$, giving rise to the *Raman lines* (see Fig. 1b). At the same time, other exciting light quanta are elastically scattered, producing the *Rayleigh line* (of frequency ν_0) with the same energy as the exciting line. The intensity of the Rayleigh line is normally several orders of magnitude larger than the Raman lines.

In Raman spectroscopy, exciting radiation from the visible part of the spectrum is usually employed. Using radiation with a frequency close to that of an electronic absorption, the *resonance Raman effect* may be observed (see Sec. 5.1). To mitigate interfering fluorescence processes, Raman spectra may be excited in the near-IR region (see Sec. 6.5).

Infrared and Raman spectroscopy are complementary tools for obtaining vibrational spectra. Depending on the nature of the vibration, which is determined by the symmetry of the molecule, vibrations may be active or forbidden in the infrared or Raman spectrum. *Infrared active* are all vibrations which modulate

the molecular dipole moment. *Raman active* are vibrations which modulate the molecular polarizability. Vibrations which are forbidden in both spectra are called *silent*. Vibrations of molecules with a center of symmetry which are infrared active cannot be Raman active and vice versa, which is the *rule of mutual exclusion*.

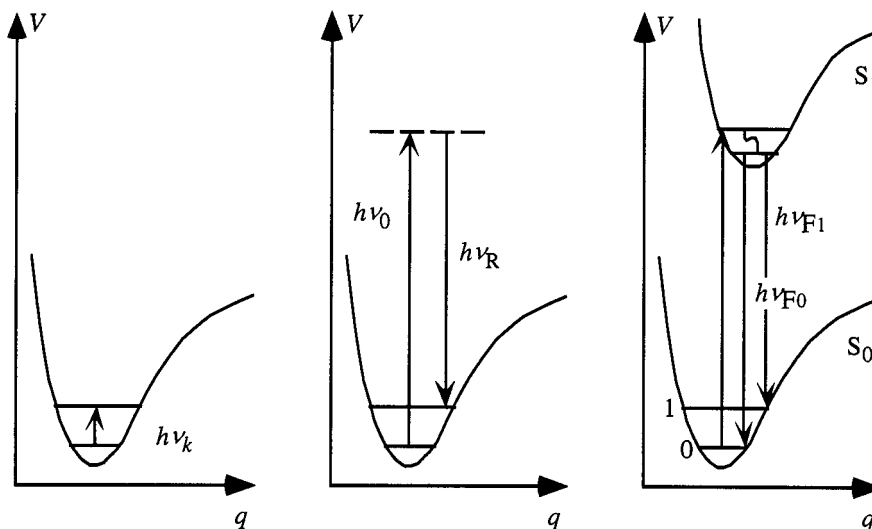


Fig. 1 a.) Infrared absorption; b.) Raman scattering; c.) fluorescence

3.3 Fluorescence

Fluorescence spectroscopy, especially of gases, may also be employed to observe molecular vibrations. (see Fig. 1c and [XVI])

4 THE RAMAN SPECTRUM

When a molecule is exposed to an electric field, electrons and nuclei are forced to move in opposite directions. A dipole moment is induced which is proportional to the electric field strength and to the *molecular polarizability* α . A molecular vibration described by the normal coordinate q_k can be observed in the Raman spectrum only if it modulates to first order the molecular polarizability [Note*]:

$$\left(\frac{\partial \alpha}{\partial q}\right)_0 \neq 0 \quad (1)$$

If the symmetry of the molecule is such that this condition is fulfilled, then the transition is said to be allowed or Raman active; if it is not fulfilled, it is said to be forbidden or *Raman inactive*.

4.1 Raman frequencies

A normal vibration is described by the normal coordinate q_k and the normal frequency ν_k :

$$q_k = q_k^0 \cos(2\pi \nu_k t) \quad (2)$$

The normal frequencies are dependent on the masses of the atoms, the elastic forces between them, the *force constants*, and the geometry of the atomic positions and may be calculated by the method of *normal*

* Note: According to the classical treatment. The quantum mechanical treatment is discussed in Ref. 1.

coordinate analysis (see Ref. 2). This method can be used to elucidate molecular structures by adjustment of molecular parameters to minimize the difference between calculated and observed frequencies.

If a molecule is put into an alternating electric field of frequency ν_0 a dipole moment p with alternating polarity at the frequency ν_0 is induced. The components of the vector of the electric field according to a molecular fixed Cartesian coordinate system are described by E_x , E_y and E_z . The *induced dipole moment* p_i can be described by its components:

$$\begin{aligned} p_x &= \alpha_{xx} E_x + \alpha_{xy} E_y + \alpha_{xz} E_z \\ p_y &= \alpha_{yx} E_x + \alpha_{yy} E_y + \alpha_{yz} E_z \\ p_z &= \alpha_{zx} E_x + \alpha_{zy} E_y + \alpha_{zz} E_z \end{aligned} \quad (3)$$

where α_{ij} are components of the *polarizability tensor* α :

$$\alpha = \begin{bmatrix} \alpha_{xx} & \alpha_{xy} & \alpha_{xz} \\ \alpha_{yx} & \alpha_{yy} & \alpha_{yz} \\ \alpha_{zx} & \alpha_{zy} & \alpha_{zz} \end{bmatrix}$$

which projects the electric field vector \vec{E} to produce the induced dipole moment vector \vec{p} . This can be written in matrix notation as:

$$\vec{p} = \alpha \vec{E}$$

$$\alpha_k = \alpha_0 + \left[\frac{\partial \alpha}{\partial q_k} \right]_0 q_k^0 \cos 2\pi \nu_k t + \dots \quad (4)$$

Equations 3 and 4 can be combined to give:

$$p_k = \alpha_0 E_0 \cos(2\pi \nu_0 t) + \frac{1}{2} \left(\frac{\partial \alpha}{\partial q_k} \right)_0 q_k^0 E_0 [\cos(2\pi(\nu_0 - \nu_k)t) + \cos(2\pi(\nu_0 + \nu_k)t)] \quad (5)$$

This oscillating *Hertzian dipole* $|\vec{p}_k|$, produces electromagnetic radiation. The first term in Eq. 5 describes Rayleigh scattering, the second term *Stokes Raman scattering*, and the third *anti-Stokes Raman scattering*. This classical equation, however, does not show the individual intensities of *Stokes* and *anti-Stokes Raman lines*.

4.2 Anharmonicity

As the molecular potential is anharmonic, the higher-order terms of the potential energy of the molecules are not negligible. This *mechanical anharmonicity* gives rise to *combination frequencies*. They are also produced by the higher terms of the polarizability, i.e. the *electrical anharmonicity* (see Eq. 4). Thus, combinations of two or more normal vibrations, i.e. overtones, sum or difference frequencies, are produced. These appear as bands in the spectra, but usually only with small intensity. Interactions of the combination frequencies with fundamentals also occur; the interaction of an overtone or combination with a fundamental of the same symmetry and nearly the same frequency is called *Fermi resonance*, which enhances the intensity of the overtone or combination at the expense of the fundamental, leading in this extreme case to two lines of nearly equal intensity.

4.3 Raman intensities

Placzek's theory (1934) describes the Raman effect quantitatively on the condition that the exciting frequency differs considerably from the frequencies of electronic as well as of vibrational transitions.

In order to describe the intensity of the Raman lines of liquids or gases the parameters α'_k and γ'_k are used. They stand for the isotropic and the anisotropic parts of the polarizability change during a normal vibration ν_k , respectively, and are given by (in order to simplify these equations, the subscript k has been omitted):

$$\alpha' = \frac{1}{3} [\alpha'_{xx} + \alpha'_{yy} + \alpha'_{zz}] \quad (6)$$

$$\gamma'^2 = \frac{1}{2} [(\alpha'_{xx} - \alpha'_{yy})^2 + (\alpha'_{yy} - \alpha'_{zz})^2 + (\alpha'_{zz} - \alpha'_{xx})^2 + 6(\alpha'^2_{xy} + \alpha'^2_{xz} + \alpha'^2_{zy})] \quad (7)$$

The terms $\alpha'_{ij} = \left[\frac{\partial \alpha_{ij}}{\partial q} \right]_0$ are the components of the *tensor of the polarizability change* resulting from a normal vibration q .

The polarizability has the dimension $J^{-1} C^2 m^2$. In the old literature the polarizability has been described as a volume, in analogy to the molecular volume ($1 \text{ \AA}^3 = 10^{-24} \text{ cm}^3$). The *polarizability volume* results when the polarizability given in SI units is divided by $4\pi\epsilon_0$ (in $J^{-1} C^2 m^{-1}$). The normal coordinates are mass weighted and have the dimension $\text{cm}^{1/2}$.

When the Raman spectrum of a liquid or a gas is measured by irradiating along the c axis with linearly polarized radiation whose electric vector is oriented in the a direction and the Raman spectrum is observed along the b axis (Fig. 2), then the c and b axis define the *plane of observation*.

The *integral Raman scattering coefficient* (the *absolute differential Raman scattering cross section* ($d\sigma/d\Omega$) in $\text{cm}^2 \text{ sr}^{-1}$) of the Stokes line (shifted to lower energies) of the k th Raman-active vibration of wavenumber $\tilde{\nu}_k$, with the electric vector of the exciting radiation oriented perpendicular to the plane of observation, is given by [Ref. 4]:

$$\left(\frac{d\sigma}{d\Omega} \right)_{k\perp} = \frac{\pi^2}{45 \epsilon_0^2} \cdot \frac{b_k^2 (\tilde{\nu}_0 - \tilde{\nu}_k)^4}{1 - \exp(-hc \tilde{\nu}_k/kT)} \cdot g_k (45 \alpha'^2_k + 7 \gamma'^2_k) \quad (8)$$

where σ is the scattering cross section, Ω is the solid angle, and g_k is the *degeneracy* of this vibration.

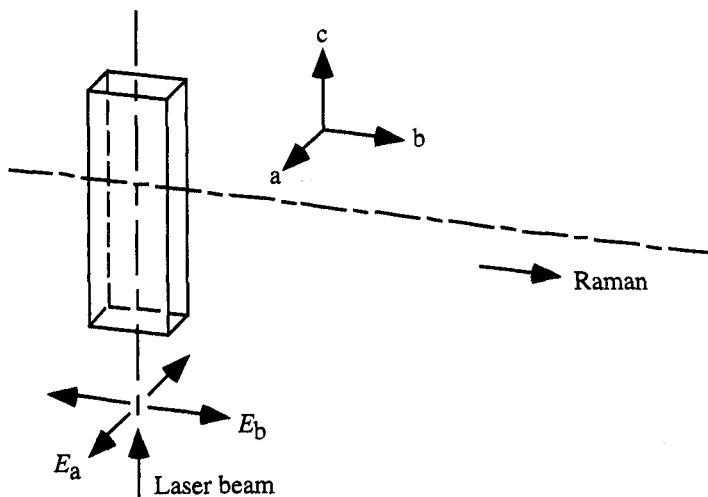


Fig. 2 Orientation of the electric vector of the exciting laserbeam to the Raman observation direction.

The expression

$$g_k \left(45 \alpha'_k{}^2 + 7 \gamma'_k{}^2 \right) \quad (9)$$

is known as the *scattering activity*, and

$$b_k^2 = h/8 \pi^2 c \tilde{\nu}_k \quad (10)$$

is the square of the *zero point amplitude* of the vibration. Eq. 8 may be simplified:

$$\left(\frac{d\sigma}{d\Omega} \right)_{k\perp}^- = \frac{h}{2^3 c \varepsilon_0^2} \cdot \frac{(\tilde{\nu}_0 - \tilde{\nu}_k)^4}{\tilde{\nu}_k [1 - \exp(-hc \tilde{\nu}_k/kT)]} \cdot g_k \left(\alpha'_k{}^2 + \frac{7}{45} \gamma'_k{}^2 \right) \quad (11)$$

This equation is valid for observation without a polarization analyzer. In order to eliminate the usual different transmission of spectrometers for radiation of different polarization orientation, an arrangement is used which allows the polarization of the exciting radiation to be switched between the *a* direction (perpendicular, \perp) and the *b* direction (parallel, \parallel) while only allowing scattered radiation with its electric vector oriented in the *a* direction (\perp to the plane of observation) to enter the spectrometer. In this case, for exciting radiation with its electric vector oriented in the *a* direction (\perp to the plane of observation), the scattering coefficient is given by:

$$\left(\frac{d\sigma}{d\Omega} \right)_{k\perp}^- = \frac{h}{2^3 c \varepsilon_0^2} \cdot \frac{(\tilde{\nu}_0 - \tilde{\nu}_k)^4}{\tilde{\nu}_k [1 - \exp(-hc \tilde{\nu}_k/kT)]} \cdot g_k \left(\alpha'_k{}^2 + \frac{4}{45} \gamma'_k{}^2 \right) \quad (12)$$

and conversely, if the electric vector of the exciting radiation is oriented in the *b* direction (\parallel to the plane of observation), then the scattering coefficient is given by:

$$\left(\frac{d\sigma}{d\Omega} \right)_{k\parallel}^- = \frac{h}{2^3 c \varepsilon_0^2} \cdot \frac{(\tilde{\nu}_0 - \tilde{\nu}_k)^4}{\tilde{\nu}_k [1 - \exp(-hc \tilde{\nu}_k/kT)]} \cdot g_k \left(\frac{3}{45} \gamma'_k{}^2 \right) \quad (13)$$

In the case of anti-Stokes Raman scattering (superscript $^+$) with the electric vector of the exciting radiation oriented in the *a* direction (\perp to the plane of observation), the scattering coefficient is:

$$\left(\frac{d\sigma}{d\Omega} \right)_{k\perp}^+ = \frac{h}{2^3 c \varepsilon_0^2} \cdot \frac{(\tilde{\nu}_0 + \tilde{\nu}_k)^4}{\tilde{\nu}_k [\exp(hc \tilde{\nu}_k/kT) - 1]} \cdot g_k \left(\alpha'_k{}^2 + \frac{4}{45} \gamma'_k{}^2 \right) \quad (14)$$

The ratio of the coefficients of the Stokes and anti-Stokes Raman lines, the *Stokes/anti-Stokes intensity ratio* is given by:

$$\left(\frac{d\sigma}{d\Omega} \right)_{k\perp}^- / \left(\frac{d\sigma}{d\Omega} \right)_{k\perp}^+ = \left(\frac{(\tilde{\nu}_0 - \tilde{\nu}_k)}{(\tilde{\nu}_0 + \tilde{\nu}_k)} \right)^4 \cdot \exp(hc \tilde{\nu}_k/kT) \quad (15)$$

This equation allows contact-free determination of sample temperature.

The equation above is valid for instruments which measure intensities of the radiation. If, however, instruments use photon counting devices, then the Stokes/anti-Stokes ratio given in Eq. 15 changes into:

$$r = \frac{n^-}{n^+} = \left(\frac{(\tilde{\nu}_0 - \tilde{\nu}_k)}{(\tilde{\nu}_0 + \tilde{\nu}_k)} \right)^3 \cdot \exp(hc \tilde{\nu}_k/kT) \quad (16)$$

where for photon counting $I \propto P = nh(\nu_0 \pm \nu_1)$, and n = the count rate [Ref. 4].

Very useful information can be derived from the intensities in spectra that are obtained as in equations 12 and 13 (i.e. with a polarization analyzer oriented along the a direction and excitation with polarization parallel and perpendicular to the plane of observation). The ratio of the two scattering coefficients is known as the *depolarization ratio* ρ :

$$\rho_k = \left(\frac{d\sigma}{d\Omega} \right)_{kl}^- / \left(\frac{d\sigma}{d\Omega} \right)_{k\perp}^- = \frac{3\gamma'_k{}^2}{45\alpha'_k{}^2 + 4\gamma'_k{}^2} \quad (17)$$

The depolarization ratio may be used to determine the symmetry of the vibrations of molecules in the liquid or gaseous state. The *depolarization ratio for totally symmetric vibrations* lies between 0 and 3/4. For cubic point groups, the depolarization ratio for totally symmetric vibrations is 0. All other vibrations have a depolarization ratio of 3/4 [Ref. 3].

Single crystals give, when their crystal axes are oriented in the direction of the axes of the instrument, up to 6 different Raman spectra, showing the activity with respect to the different symmetry species of the vibrations of the unit cell. Their orientation is described by the *Porto notation* [Ref. 4], $a(bc)d$, where a is the direction of the exciting radiation with electric vector oriented in the b direction and, with an analyzer transmitting radiation with an electric vector parallel to the c direction, the radiation emerging in the d direction is measured.

5 NON-CLASSICAL RAMAN EFFECTS

5.1 Resonance Raman effect

Resonance Raman spectroscopy (RRS) makes use of an excitation source with frequency close to a molecular electronic absorption frequency. Under these conditions a resonance occurs which may enhance the intensities of the Raman lines by several orders of magnitude, especially those connected with totally symmetric vibrations of the chromophore. (Fig. 3)

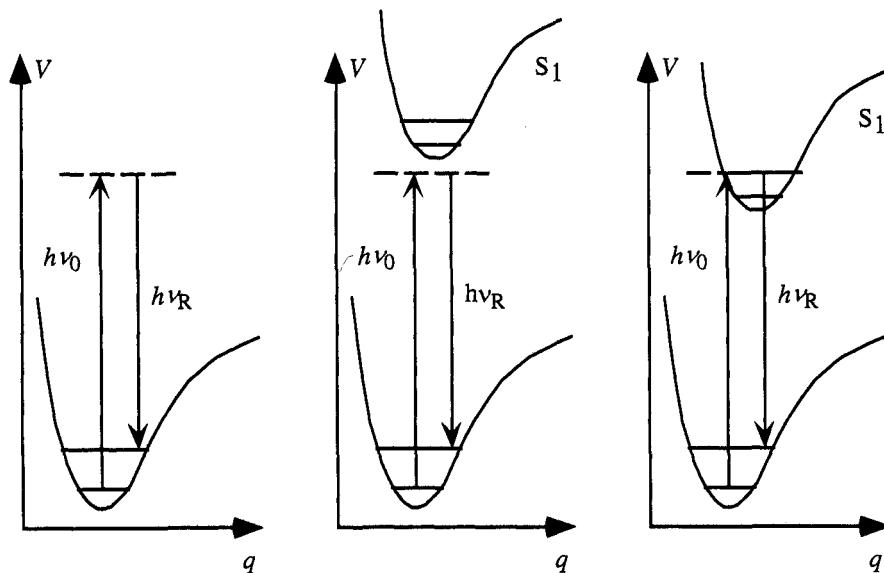


Fig. 3 a.) Raman scattering; b.) near-resonance Raman; c.) resonance Raman

5.2 Surface-enhanced Raman effect

The influence of small metal (silver, gold, copper) particles such as colloids or roughened surfaces on the elementary process of Raman scattering can enhance the intensity of the Raman effect by several orders of magnitude. This effect is used in *surface-enhanced Raman spectroscopy* (SERS).

Resonance and surface-enhanced Raman effects may be combined to produce *surface-enhanced resonance Raman spectroscopy* (SERRS).

RRS, SERS, and SERRS can be recorded with the same spectrometers as classical Raman spectra, although different conditions of the excitation and special sample techniques are used. They are important techniques for trace chemical analyses.

5.3 Non-linear Raman effects

If the exciting radiation has a very high intensity, then the higher terms of the polarizability expansion have to be considered:

$$p = \alpha \bar{E}_i + \frac{1}{2} \beta \bar{E}_i \bar{E}_j + \frac{1}{6} \gamma \bar{E}_i \bar{E}_j \bar{E}_k + \dots \quad (18)$$

where β is the 1st molecular hyperpolarizability, and γ is the 2nd molecular hyperpolarizability, leading to non-linear Raman effects.

Hyper-Raman scattering is produced by very high intensity pulses. Two photons of the exciting radiation produce the Raman spectrum.

With two or three laser beams of different frequency, different coherent Raman effects may be observed. Fig. 4 describes the most important of these effects: *coherent Stokes Raman spectroscopy*, CSRS; *coherent anti-Stokes Raman spectroscopy*, CARS; *stimulated Raman gain spectroscopy*, SRGS; inverse Raman spectroscopy, IRS or *stimulated Raman loss spectroscopy*, SRLS [Note*]; and *photoacoustic Raman spectroscopy*, PARS.

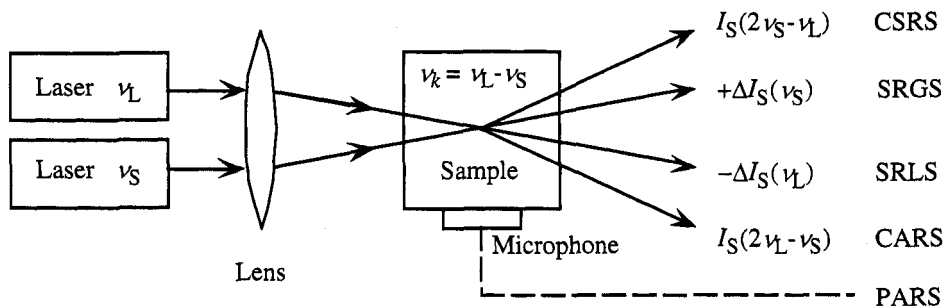


Fig. 4 The most analytically useful coherent Raman effects (after Kiefer in Ref. 3, p.168)

6. RECORDING OF RAMAN SPECTRA

6.1 Raman spectrometers

The radiant flux through a spectrometer is (see [I, appendix B]):

$$\Phi = L \bar{\nu} G \bar{\nu} (\Delta \bar{\nu})^2 \tau \quad (19)$$

* Note: Stimulated Raman loss spectroscopy is the recommended term.

with $L\tilde{\nu}$, the *spectral radiance* and $G\tilde{\nu}$ the *spectral optical conductance*, $\Delta\tilde{\nu}$ the *spectral bandwidth* [XVI 2.1], and τ the *transmission factor* of the instrument [IX 4.2]. The *spectral optical conductance of a grating spectrometer* [IX 7.3.4] is approximately:

$$GG_{\tilde{\nu}} \approx \frac{hA_G}{f\tilde{\nu}} \quad (20)$$

where A_G is the *beam area* at the grating of the spectrometer, h is the *slit length* of the grating spectrometer and f is the *collimator focal length* [IX 4.1]. The *spectral optical conductance of a Michelson interferometer* is given by:

$$GL_{\tilde{\nu}} \approx \frac{2\pi A_I}{\tilde{\nu}} \quad (21)$$

where A_I is the *beam area* at the beamsplitter of the interferometer. The ratio of both equations is:

$$GL_{\tilde{\nu}} / GG_{\tilde{\nu}} = \frac{2\pi f}{h} \frac{A_I}{A_G} \quad (22)$$

When $A_I = A_G$, this ratio is called the *Jacquinot advantage*. As the slit height of a grating spectrometer is usually about 1/50 of the focal length, this ratio is about 300. This means that interferometers may transport a considerably larger radiation flux to the detector than grating spectrometers.

When a grating spectrometer is used with an array detector, a manifold of exit slits are in principle acting simultaneously. This is the basis of the *multichannel advantage* of such instruments. Interferometers use one detector element to measure the intensities of many spectral channels simultaneously. If the detector is the main source of noise, then the *signal to noise ratio* r_{SN} (XI Table 1) is increased relative to a single channel instrument proportionally to the square root of the number of spectral channels - the *multiplex advantage*.

6.2 The radiant power of Raman scattered radiation

The differential Raman scattering cross section is proportional to the fourth power of the emitted frequency, the ν^4 factor. Dividing Eq. 8 by $(\tilde{\nu}_{\text{ref}} - \tilde{\nu}_k)^4$, gives the *absolute normalized Raman scattering cross section* (Eq. 23) of a Raman line with frequency shift ν_k . [Ref. 3]

$$\left(\frac{d\sigma}{d\Omega}\right)_{k\perp}^{-1} \cdot (\tilde{\nu}_{\text{ref}} - \tilde{\nu}_k)^{-4} = \frac{h}{2^3 c \epsilon_0^2} \cdot \frac{g_k}{\tilde{\nu}_k [1 - \exp(-hc\tilde{\nu}_k/kT)]} \cdot \left(\alpha' \frac{2}{k} + \frac{7}{45} \gamma' \frac{2}{k}\right) \quad (23)$$

where $\tilde{\nu}_{\text{ref}}$ is the *reference excitation wavenumber* (see Ref. 5). The right-hand side of Eq. 23 represents the microscopic parameters of the sample and has been tabulated for a number of gases and liquids and for several $\tilde{\nu}_{\text{ref}}$ in Ref. 5. According to Placzek's theory, this expression should be independent of the frequency of the exciting radiation in the absence of a resonance or near-resonance Raman effect. The term on the left-hand side normalizes the observed Raman intensity by including the ν^4 factor.

The radiant power of the observed radiation is proportional to the absolute normalized Raman scattering cross section, i.e. to the ν^4 factor and to the *number of molecules per unit volume* N . The *Raman scattering coefficient* s_R of this line is thus:

$$s_R = \left(\frac{d\sigma}{d\Omega}\right)_{k\perp}^{-1} \cdot (\tilde{\nu}_{\text{ref}} - \tilde{\nu}_k)^{-4} (\tilde{\nu}_0 - \tilde{\nu}_k)^4 N L_n \quad (24)$$

where L_n is the internal field factor:

$$L_n = (n_R/n_0)(n_R^2+2)^2(n_0^2+2)^2/3^4 \quad (25)$$

and n_0 and n_R are the refractive indices of the scattering medium at the wavelength of the exciting and the Raman radiation, respectively, which takes into account the increase of the incident and scattered electric field due to the dielectric nature of the scattering medium.

The *radiance of a Raman line* L_R (scattered power per unit solid angle per unit area of sample integrated over the Raman line in question) is proportional to the radiant power of the exciting radiation divided by the cross sectional beam area $r^2 \pi$ and multiplied by the Raman scattering coefficient:

$$L_R = \frac{\Phi_0}{r^2 \pi} d s_R \quad (26)$$

where d is the *sample thickness* of the observed sample, and r is the beam radius [XV].

6.3 Influence of the optical properties of the sample

For chemical analysis, a sample arrangement should make it possible to record Raman spectra within a short time period with a high signal to noise ratio r_{SN} [XI Table 1] using a small amount of substance (small sample). To optimize the sample arrangement one must enhance the measured intensity of the Raman radiation produced by a given radiant power of the laser radiation. It is of the utmost importance to take into account and make proper use of the optical properties of the sample.

The *Kubelka–Munk theory* can be extended to describe the Raman scattering of crystal powders, liquids, and transparent solids (Ref. 6). This theory considers one surface of a layer with thickness d irradiated homogeneously with radiant intensity I_0 . I and J are the radiation intensities emerging from the surfaces with the subscripts P and R representing, respectively, unshifted (primary) and Raman radiation. A parameter k is introduced:

$$k^2 = 2r\alpha + \alpha^2 \quad (27)$$

where α is the linear Napierian absorption coefficient and r is the linear Napierian scattering coefficient. [Ref. 7]

For chemical analysis it is particularly important to know the *transmitted Raman-to-unshifted intensity ratio* (i.e. in the 0° arrangement): [Refs. 3, 6]

$$\frac{I_R}{I_P} = \frac{s k^2 d - r + (\alpha+r)kd \coth kd}{\alpha + r + k \coth kd} \quad (28)$$

and *back-scattered Raman-to-unshifted intensity ratio* (i.e. in the 180° arrangement):

$$\frac{J_R}{J_P} = \frac{s k}{r \alpha} \frac{k \sinh kd + (\alpha+r) \cosh kd - \frac{k r d}{\sinh kd}}{(\alpha+r) \sinh kd + k \cosh kd} \quad (29)$$

where s is the linear *Napierian Raman scattering coefficient*, and I and J are the forward and back-scattered intensities of the unshifted (subscript P) and Raman (subscript R) radiation at the frequencies $\tilde{\nu}_0$ and $\tilde{\nu}_k$, respectively, see Fig. 5.

In classical Raman spectroscopy, Raman spectra are recorded from colorless samples with exciting radiation in the visible range of the spectrum. In this case, α is of the order of 10^{-3} to 10^{-5} cm^{-1} . However, in the near infrared (NIR) range, α may be of the order 10^{-1} – 10^2 cm^{-1} because of the overtones and combinations of the X-H stretching vibrations (where X may be any element).

The scattering coefficient for crystal powders is approximately inversely proportional to the diameter of the particles. For coarse, medium and fine powders, r is approximately 10, 100, and 1000 cm^{-1} , respectively. In the case of pure liquids, solutions, fibers, and single crystals, r is approximately 0.

Figs. 5 a.) and b.) show the relative intensities J_R and I_R of the Raman radiation of samples with different thicknesses in the back-scattering and the forward-scattering arrangement. Figs. 5 c.) and d.) show the reflectance ρ and the transmittance τ of the exciting radiation, with $J_P/I_0 = \rho$ and $I_P/I_0 = \tau$. The Raman scattering coefficient is assumed to be equal for all samples. Only relative intensities of the Raman spectrum are discussed.

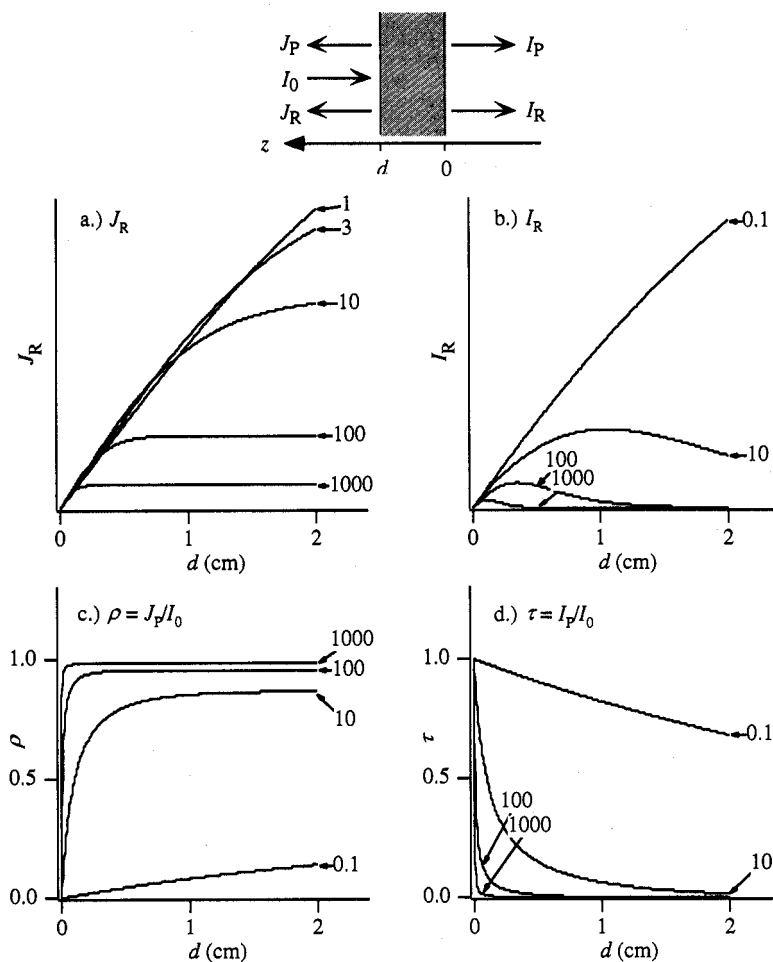


Fig. 5 Plots of the forward (I) and backscattered (J), unshifted (P) and Raman (R) intensities versus sample thickness d and at several values of r , for $\alpha = 0.1 \text{ cm}^{-1}$. The incident intensity is I_0 . Plot a.) is of J_R the back-scattered Raman intensity; b.) is of I_R , the forward-scattered Raman intensity; c.) is of ρ , the reflectance of the Rayleigh radiation; and d.) is of τ , the transmittance of the Rayleigh radiation.

6.3.1 Liquid samples

Liquids can be assumed to be samples with an elastic scattering coefficient approaching 0. The diagrams for $r = 0$ show that in the back-scattering arrangement (Fig. 5 a), the intensities of the Raman lines increase with the sample thickness. Fig. 5 c.) demonstrates that under the same conditions the intensity of unshifted radiation is very low. In the forward scattering arrangement, however, the intensity of the Raman lines also increases with the thickness of the sample (Fig. 5 b), but the Raman radiation is mixed with a very large

amount of unshifted radiation (Fig. 5 d). Thus, liquids are best investigated with a back-scattering arrangement with a large effective thickness.

6.3.2 Powder samples

Coarse, medium, and fine crystal powders have an elastic scattering coefficient of about 10, 100, or 1000 cm^{-1} , respectively. With the back-scattering arrangement (Fig. 5 a), the intensity of the Raman lines increases with the thickness of the sample. In the case of fine powders ($r = 1000 \text{ cm}^{-1}$), this intensity reaches a small limiting value at a small thickness. For larger grains ($r = 10$ or 100 cm^{-1}), a higher limiting value is reached at a larger thickness. The same samples show a reflectance (Fig. 5 c) which approaches, for larger scattering coefficients, higher limiting values at smaller thicknesses. The limiting value for $r = 1000 \text{ cm}^{-1}$ is $\rho = 98.6 \%$; for $r = 100 \text{ cm}^{-1}$, $\rho = 95.6 \%$; and for $r = 10 \text{ cm}^{-1}$, $\rho = 87.8 \%$.

Therefore, the low intensity of the Raman radiation can be considerably enhanced by utilizing multiple reflections of the exciting and the emerging Raman radiation both in the sample and using an external spherical mirror. Thus *multiple reflection arrangements* may have a high efficiency which is nearly independent of the size of the grains!

Fig. 5 b.) shows the intensity of the Raman radiation using a forward-scattering arrangement. At an *optimum sample thickness* d_{opt} , the Raman radiation has a maximum which increases as the elastic scattering coefficient decreases. The exciting radiation which emerges from the sample (Fig. 5 d) decreases in intensity with increasing elastic scattering coefficient.

Compared to back-scattering arrangements, forward-scattering arrangements produce lower absolute intensities of the Raman lines. However, the ratio of the Raman line intensity relative to the intensity of the exciting radiation emerging from the sample exceeds that of a back-scattering arrangement by one or two orders of magnitude. Thus, the optimum sample arrangement for Raman spectroscopy of crystal powders with a low absorption coefficient is a *forward-scattering (0°) multiple reflection arrangement* of coarse crystallites with an optimum sample thickness. In the case of relatively high absorption coefficients, as in NIR-excited Raman spectroscopy, coarse powders should be investigated with a back-scattering (180°) multiple reflection arrangement.

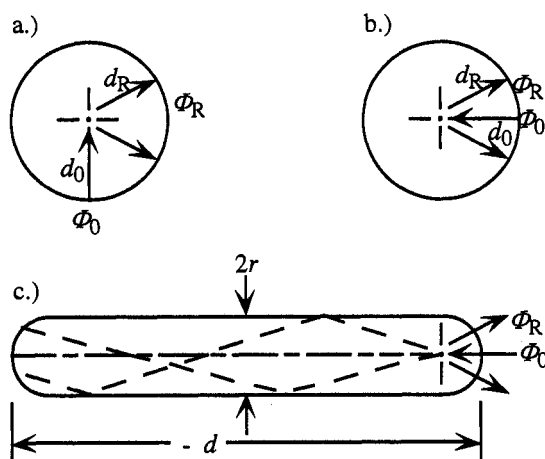


Fig. 6 Liquid sample arrangements: a.) perpendicular-scattering (90°) arrangement in a spherical cell, b.) back-scattering (180°) arrangement in a spherical cell, and c.) back-scattering arrangement through the spherical bottom of a capillary cell (see ref. 1).

6.4 Influence of thermal emission

Especially for Raman spectroscopy with excitation in the NIR range, thermal emission, due to heating of the sample for the laser radiation, may interfere with the detection of the Raman signals. The *Planck-Kirchhoff law* determines the spectral radiance of a sample with a molar decadic absorption coefficient ε at a wavenumber $\tilde{\nu}$ and a temperature T :

$$L_{\tilde{\nu},T} = \frac{2hc\tilde{\nu}^3}{\exp(hc\tilde{\nu}/kT) - 1} \left(1 - 10^{-\varepsilon(\tilde{\nu})Cd} \right) \quad (30)$$

where c is the speed of light in vacuum and C is the molar concentration of substance.

6.5 Influence of fluorescence and phosphorescence

Even small amounts of contaminant or nascent fluorescent species can produce fluorescence that masks the Raman spectrum of a sample because typical fluorescence cross sections are 10^6 times larger than Raman cross sections. Shifting the excitation frequency to lower energies, so that electronic excitation of sample or contaminants is avoided, is an appropriate method to reduce fluorescence interference. Excitation using Nd:YAG [see XV] radiation at 1064 nm has proven to be useful in this context. The strong dependence on the ν^4 factor causes a reduction of the Raman intensity compared to visible excitation. This disadvantage can be compensated using the Jacquinot and multiplex advantages of interferometers [see IX].

6.6 Special sample arrangements

6.6.1 Non-absorbing powders

For non-absorbing crystal powders, the forward-scattering multiple reflection arrangement is superior to other arrangements because it combines a high scattered intensity of the Raman radiation with the maximum transmitted Raman to excitation intensity ratio.

6.6.2 Absorbing samples

Absorbing samples – as in the case of *NIR-excited Raman spectroscopy* – should be measured using a 180° *back-scattering multiple reflection arrangement*. Often interferometers are employed, which have a circular entrance aperture, the *Jacquinot stop*, instead of an entrance slit as in a grating spectrometer. The 180° back-scattering arrangement is therefore recommended for three reasons: 1) the intensities observed under these conditions are the highest; 2) the exciting radiation irradiates a conical volume of the sample (the Raman radiation emerging from this volume irradiates optimally the beam splitter of the interferometer through the circular Jacquinot stop); and 3) a circular spot is more aberration-tolerant than a line of the same area and thus can be demagnified further. [Ref. 5]

Use of a *spherical cuvette* will improve the detected fraction of the Raman signal versus a rectangular cuvette. The foci are not blurred, the effective solid angle of the collected Raman radiation is equal to that of the sample optics, and the reflection losses are small and equal because for every ray $\Theta = 0$. The necessary amount of sample is about the size of the focal region of the exciting laser beam. The sample at the focus of the laser beam may be effectively cooled if the sphere is made from a material which has a high thermal conductance, such as sapphire.

6.7 Presentation of Raman spectra

It is recommended that Raman spectra be presented with a linear abscissa scale in wavenumbers (cm^{-1}) increasing from the right to the left. In this way, Raman spectra can be compared better to the complementary infrared spectra. However, the ordinate scale should be drawn linearly increasing from bottom to top with relative or preferably absolute intensity units.

7 INDEX OF TERMS

Term	Section	Term	Section
absolute differential Raman scattering		1 st molecular polarizability β	5.3
cross section ($d\sigma/d\Omega$)	4.3	2 nd molecular hyperpolarizability γ	5.3
absolute normalized Raman scattering		multichannel advantage	6.1
cross section	6.2	multiple diffraction of powders	1.2
anti-Stokes Raman lines	4.1	multiple reflection of powders	1.2
anti-Stokes Raman scattering	4.1	multiple refraction of powders	1.2
anti-Stokes Raman spectrum	1.1	multiplex advantage	6.1
atomic mass m	2.1	Napierian Raman scattering	
back-scattered Raman to excitation		coefficient s	6.3
intensity ratio J_R/J_P	6.3	Napierian absorption coefficient α	6.3
back-scattering multiple reflection		Napierian scattering coefficient r	6.3
arrangement	6.6.2	NIR-excited Raman spectroscopy	6.6.2
beam area A	6.1	non-linear Raman effects	5.3
Brillouin scattering	1.2	normal coordinate q_k	2; 4.1
coherent anti-Stokes Raman scattering		normal coordinate analysis	4.1
(CARS)	5.3	normal frequency ν_k	2; 4.1
coherent Stokes Raman scattering		normal vibration k	2; 4.1
(CSRS)	5.3	ν^4 factor	6.2
collimator focal length f	6.1	optimum sample thickness d_{opt}	6.3.2
combination frequencies	4.2	overtones	4.2
degeneracy g_k	4.3	phosphorescence	1.2
depolarization ratio ρ	4.3	photo-acoustic Raman spectroscopy	
depolarization ratio for totally symmetric		(PARS)	5.3
vibrations	4.3	photoluminescence	1.2
delayed fluorescence	1.2	Placzek's theory	4.3
difference frequencies	4.2	plane of observation	4.3
diffuse reflection	1.2	Planck-Kirchhoff law	6.4
diffuse scattering	1.2	polarizability volume	4.3
Doppler effect	1.2	Porto notation	4.3
elastic scattering process	1.2	primary light quantum	1.2
electrical anharmonicity	4.2	radiance of a Raman line L_R	6.2
excitation source	3.2	Raman active vibrations	3.2
exciting radiation	3.2	Raman effect	1.2
Fermi resonance	4.2	Raman lines	3.2
fluorescence	1.2	Rayleigh line	3.2
force constants	4.1	Rayleigh scattering	1.2
forward-scattering multiple reflection		reference excitation wavenumber $\tilde{\nu}_{ref}$	6.2
arrangement	6.3.2	reflectance of the exciting radiation ρ	6.3
Hertzian dipole	4.1	resonance Raman effect	3.2
hyper Raman scattering	5.3	resonance Raman spectroscopy (RRS)	5.1
induced dipole moment μ_i	4.1	rotation-vibration Raman spectrum	1.2
inelastic scattering process	1.2	rotational Raman spectrum	1.2
infrared absorption spectrum	3.1	rotational energy E_{rot}	1.2
infrared active vibrations	3.2	rotational temperature	1.2
integral Raman scattering coefficient	4.3	rule of mutual exclusion	3.2
internal field factor L_n	6.2	sample thickness d	6.2
Jacquinot advantage	6.1	scattering activity	4.3
Kubelka-Munk theory	6.3	scattering process	1.2
laser Doppler anemometry	1.2	secondary light quantum	1.2
mechanical anharmonicity	4.2	signal to noise ratio r_{SN}	6.1
Mie scattering	1.2	silent vibrations	3.2
molecular polarizability α	4	slit length h	6.1

solid angle Ω	6.1	(SERS)	5.3
spectral radiance $L_{\tilde{\nu}}$	6.1	surface-enhanced resonance Raman	
spectral optical conductance $G_{\tilde{\nu}}$	6.1	spectroscopy (SERRS)	5.3
spectral optical conductance of a grating spectrometer $G_{\tilde{\nu}}^{G_{\nu}}$	6.1	tensor of the polarizability change	4.3
spectral optical conductance of a Michelson interferometer $G_{\tilde{\nu}}^I$	6.1	transmission factor τ	6.1
spherical cuvette	6.6.2	transmittance of the exciting radiation τ	6.3
stimulated Raman gain spectroscopy (SRGS)	5.3	transmitted Raman to excitation intensity ratio I_R/I_p	6.3
stimulated Raman loss spectroscopy (SRLS)	5.3	Tyndall scattering	1.2
Stokes/anti-Stokes intensity ratio	4.3	vibrational energy E_{vib}	1.2
Stokes Raman lines	4.1	vibrational modulation of the polarizability	4.1
Stokes Raman scattering	4.1	vibrational Raman spectrum	1.2
Stokes Raman spectrum	1.2	vibrational temperature	1.2
sum frequencies	4.2	wavenumber	3.1
surface-enhanced Raman spectroscopy		zero-point amplitude b_k	4.3

8 REFERENCES

- 1 D.A. Long. *Raman Spectroscopy*, (McGraw Hill, 1977).
- 2 E.B. Wilson, J.C. Decius, P.C. Cross. *Molecular Vibrations, The Theory of Infrared and Raman Vibrational Spectra*, (McGraw Hill, NY, 1955).
- 3 B. Schrader. *Vibrational Spectroscopy - Methods and Application*, (VCH, Weinheim, 1995).
- 4 B.J. Kip, R.J. Meier. *Appl. Spectrosc.* **44**, 707 (1990); F. LaPlant, G. Laurence, and D. Ben-Amotz, *Appl. Spectrosc.* **50**, 1034 (1996).
- 5 H. W. Schrötter, H. W. Klöckner, in *Raman Spectroscopy*, edited by A. Weber (Springer, Berlin, 1974) Ch. 4.
- 6 B. Schrader, G. Bergmann. *Fresenius. Z. Anal. Chem.* **225**, 230 (1967).
- 7 *Quantities, Units, and Symbols in Physical Chemistry*, prepared by I.M. Mills *et al.*, (Blackwell, Oxford, 1993) [known as the IUPAC "Green Book"].
- 8 T. Hirschfeld. *Appl. Spectrosc.* **31**, 289 and 471 (1977).

Table XVIII. 1 Symbols, definitions and units for Raman spectroscopy

Term	Symbol	Definition	SI unit
absolute differential Raman scattering cross section		$\left(\frac{d\sigma}{d\Omega}\right)_{kL}^{-} = \frac{\pi^2}{45 \varepsilon_0^2} \cdot \frac{b_k^2 (\tilde{\nu}_0 - \tilde{\nu}_k)^4}{1 - \exp(-hc \tilde{\nu}_k/kT)} \cdot g_k \left(45 \alpha'_k{}^2 + 7 \gamma'_k{}^2\right)$	$\text{m}^2 \text{sr}^{-1}$
absolute normalized Raman scattering cross section		$\left(\frac{d\sigma}{d\Omega}\right)_{kL}^{-} \cdot (\tilde{\nu}_{\text{ref}} - \tilde{\nu}_k)^{-4} = \frac{h}{2^3 c \varepsilon_0^2} \cdot \frac{g_k}{\tilde{\nu}_k [1 - \exp(-hc \tilde{\nu}_k/kT)]} \cdot \left(\alpha'_k{}^2 + \frac{7}{45} \gamma'_k{}^2\right)$	$\text{m}^2 \text{sr}^{-1}$
back-scattered Raman-to-unshifted intensity ratio	J_R/J_P	$= \frac{s k}{r \alpha} \frac{k \sinh kd + (\alpha + r) \cosh kd - \frac{kr d}{\sinh kd}}{(\alpha + r) \sinh kd + k \cosh kd}$	1
1 st molecular			

hyperpolarizability	β		$\text{C m}^3 \text{V}^{-2}$
2 nd molecular hyperpolarizability	γ		$\text{C m}^4 \text{V}^{-3}$
depolarization ratio	ρ_k	$= \left(\frac{d\sigma}{d\Omega} \right)_{k\parallel}^- / \left(\frac{d\sigma}{d\Omega} \right)_{k\perp}^- = \frac{3 \gamma_k'^2}{45 \alpha_k'^2 + 4 \gamma_k'^2}$	1
fundamental frequencies	ν_k		s^{-1}
induced dipole moment	μ_i		C m
internal field factor	L_n	$= (n_R/n_0)(n_R^2+2)^2(n_0^2+2)^2/3^4$	1
molecular polarizability	α		$\text{J}^{-1} \text{C}^2 \text{m}^2$ or $\text{C m}^2 \text{V}^{-1}$
Napierian absorption coefficient	α		m^{-1}
Napierian scattering coefficient	r		m^{-1}
Napierian Raman scattering coefficient	s		m^{-1}
normal coordinate	q_k		$\text{m g}^{1/2}$
normal frequency	ν_k		s^{-1}
optical conductance	G		$\text{m}^2 \text{sr}$
optimum sample thickness	d_{opt}		m
radiance of a Raman line	L_R	$= \frac{\Phi_0}{r^2 \pi} d s_R$	$\text{W sr}^{-1} \text{m}^{-2}$
Raman scattering coefficient	s_R	$= \left(\frac{d\sigma}{d\Omega} \right)_{k\perp}^- \cdot (\tilde{\nu}_{\text{ref}} - \tilde{\nu}_k)^{-4} (\tilde{\nu}_0 - \tilde{\nu}_k)^4 N L_n$	$\text{m}^{-1} \text{sr}^{-1}$
reflectance of the exciting radiation	ρ	$= J_p/I_0$	1
scattering activity	g_k	$(45 \alpha_k'^2 + 7 \gamma_k'^2)$	1
Stokes/anti-Stokes			
intensity ratio		$\left(\frac{d\sigma}{d\Omega} \right)_{k\perp}^- / \left(\frac{d\sigma}{d\Omega} \right)_{k\perp}^+ = \left(\frac{(\tilde{\nu}_0 - \tilde{\nu}_k)}{(\tilde{\nu}_0 + \tilde{\nu}_k)} \right)^4 \cdot \exp(hc \tilde{\nu}_k/kT)$	1
transmittance of the exciting radiation	τ	$= I_p/I_0$	1
transmitted Raman-to-			
unshifted intensity ratio	I_R/I_p	$= \frac{s k^2 d - r + (\alpha+r)kd \coth kd}{\alpha + r + k \coth kd}$	1
vibrational energy	E_{vib}	$= h\nu_k$	J
wavenumber	$\tilde{\nu}$	$= \nu/c$	m^{-1}
zero-point amplitude	b_k	$b_k^2 = h/8 \pi^2 c \tilde{\nu}_k$	m